

THE EFFECT OF HARDNESS OF SLIDING BODIES ON THE WEAR REGIME TRANSITION OF STEELS¹

Cristian C. Viáfara²
Amilton Sinatorá²

Abstract

This paper aims to investigate the effect of varying the hardness of both sliding bodies on the operating wear regime. Studying this behavior it is possible to obtain new insights about the origin of the wear regime transition. Unlubricated sliding wear tests were performed using a pin-on-disk configuration. The pin and disk materials were a low alloy and a tool steel, respectively. The friction force was monitored during the wear tests and the variation of mass loss of bodies as a function of sliding time was obtained to estimate the steady state wear rate. The characterization of worn surfaces was carried out using stereoscopy and scanning electron microscopy (SEM) methods, in addition to surface roughness. The results showed that the operation of mild and severe wear regimes was influenced by the initial hardness of materials. At the high pin hardness (*hph*) conditions, a decrease in the disk hardness promoted the severe wear regime operation prior to the action of a mild wear regime. At the low pin hardness (*lph*) conditions, a severe wear regime was observed that with increasing the disk hardness resulted in the wear regime transition from severe to mild.

Key-words: Wear regime transition; Sliding wear; Severe wear; Mild wear.

EFEITO DA DUREZA DOS CORPOS DESLIZANTES SOBRE A TRANSIÇÃO NO REGIME DE DESGASTE DOS AÇOS

Resumo

Este trabalho visa pesquisar o efeito da variação da dureza dos corpos deslizantes sobre a operação dos regimes de desgaste. O estudo deste tópico permite obter novas idéias sobre a origem da transição no regime de desgaste. Os ensaios de desgaste por deslizamento a seco foram executadas na configuração pino-sobre-disco. Os materiais do pino e do disco foram um aço de baixa liga e um aço ferramenta, respectivamente. A força de atrito foi monitorada durante os ensaios de desgaste e a variação das perdas de massa dos corpos em função do tempo deslizado foram obtidas para estimar a taxa de desgaste nos regimes permanentes. A caracterização das superfícies desgastadas foi realizada usando os microscópios estereoscópico e eletrônico de varredura (SEM), junto com um rugosímetro. Os resultados evidenciaram que a operação dos regimes moderado e severo de desgaste foi influenciada pela dureza inicial dos materiais. Nas condições de dureza do pino alta (*hph*), uma diminuição na dureza do disco promoveu a operação de um regime severo antes do regime moderado de desgaste. Nas condições de dureza do pino baixa (*lph*), foi observado um regime severo que com o aumento da dureza do disco resultou na transição no regime de desgaste para moderado.

Palavras chave: Transição no regime de desgaste, Desgaste por deslizamento, Desgaste severo, Desgaste moderado.

¹ Technical contribution to the First International Brazilian Conference on Tribology – TribobR-2010, November, 24th-26th, 2010, Rio de Janeiro, RJ, Brazil.

² Surface Phenomena Laboratory, Mechanical Engineering Department, Polytechnic School of the University of São Paulo.

1 INTRODUCTION

The unlubricated sliding wear of steels frequently involves the action of two main wear mechanisms: adhesive and oxidative wear.⁽¹⁾ Steady state wear regimes are promoted by these mechanisms, which are called severe and mild wear as a consequence of their wear rates produced, respectively.⁽²⁾ A complete characterization of wear regimes was carried out in the 50s⁽¹⁻³⁾ and has been confirmed in more recent works.⁽⁴⁻⁶⁾ The most interesting and relevant distinction between both wear regimes is the fact that they exhibit differences in wear rates in as much as three orders of magnitude.⁽³⁾

Wear regime transitions can be found with a slight variation in any factor of the tribological conditions such as the normal load, the sliding velocity, the hardness of bodies, among others. Another kind of wear regime transition is that occurring during the sliding process, where a transition from severe to mild wear, or vice versa, appears for a critical sliding time or distance.⁽⁷⁾ This transition has been observed with the change of normal load,⁽⁷⁾ the addition of oxide particles⁽⁸⁻¹¹⁾ and the removal of wear debris.⁽¹²⁾ A transition occurring at low values of normal load or sliding velocity was called T_1 by Welsh⁽¹³⁾ and has been observed by varying the surface roughness,⁽³⁾ the atmospheric temperature,^(14,15) the materials hardness⁽¹⁶⁾ and the relative humidity.^(17,18)

In an earlier work we found the T_1 transition from mild to severe wear when the hardness of the harder body was diminished.⁽⁵⁾ This result showed that not only the hardness of the softer body influences the tribological behavior, but too the hardness of the harder body. In the present paper we study the effect of hardness of both sliding bodies on wear regime transition of steels.

2 EXPERIMENTAL PROCEDURE

A pin-on-disk configuration was used to conduct the unlubricated sliding wear tests. Diameters of 76.2 and 4.9 mm were employed for the disk and the pin, respectively. The pin was pressed against the disk through a pneumatic system with a normal load of 35 N. A rotation speed of 40 rpm and a radius of track of 25 mm result in a sliding velocity of 0.1 m/s. A sliding time of 3600 s was sufficient to guarantee the operation of a steady state wear regime after the running-in period. The ambient temperature was $26 \pm 4^\circ\text{C}$ and the relative humidity was $41 \pm 3\%$. The initial R_q values were of $0.24 \pm 0.01 \mu\text{m}$ for the pins and $0.53 \pm 0.08 \mu\text{m}$ for the disks. The variation of the friction force was used as an indicative of the running-in and the steady state wear regime operation. For some test conditions (see Table 1), interrupted and restarted tests were performed to evaluate the mass loss of bodies as a function of the sliding time. In this way, an estimate of wear rates was made from linear regressions of the total mass loss of bodies (pin and disk).

Low alloy (AISI 4140) and tool (AISI H13) steels were employed as pin and disk materials, respectively. The low alloy steel was used with tempered martensite and bainite microstructures, which result in two levels of pin hardness. A tempered martensite microstructure was obtained in the tool steel, acquired by quenching and tempering treatments. Six levels of disk hardness were achieved by varying time and temperature of the tempering treatment. Two sets of tests were performed, where three levels of disk hardness were tested by each condition of pin hardness. The values of hardness of bodies together with test conditions are listed in Table 1. The

test condition name consists in the acronym of the low and high pin hardness (*lph* and *hph*), together with the value of the disk hardness to pin hardness ratio.

Table 1. Values of hardness of sliding bodies and test conditions

Pin hardness [HV]	Disk Hardness [HV]	Test condition
318 ± 16	356 ± 5	<i>lph1.1</i> *
	387 ± 3	<i>lph1.2</i> *
	424 ± 4	<i>lph1.3</i>
436 ± 7	460 ± 5	<i>hph1.1</i> *
	510 ± 7	<i>hph1.2</i> *
	569 ± 4	<i>hph1.3</i>

* Interrupted and restarted tests were performed in these conditions.

The worn surfaces were characterized by means of surface roughness, stereoscopy and scanning electron microscopy (SEM) techniques. R_q values and roughness profiles were obtained for comparative purposes. The pins worn surfaces were selected for the characterization due to their better representation of the wear behavior of the tribological system.

3 RESULTS

3.1 Low Pin Hardness

Figure 1(a) presents the curves of friction force as a function of sliding time for the *lph1.1* condition. The curves exhibit running-in and steady state regime periods. The duration of running-in period was always lower than 300 s.⁽¹⁹⁾ After the running-in period, a steady state regime in friction was obtained, where the mean value was close to 25 N. It can be also noted that a high variation of friction force was produced, which could be seen as an indicative of the strong asperities interaction during the sliding process and suggests the presence of the stick-slip phenomena.

Figure 1(b) presents the variation of mass loss of bodies with the sliding time for the *lph1.1* condition. This graph shows that both replicas exhibit a similar behavior, with mass loss of pins and disks being approximately the same. The mass loss behavior suggests that a steady state wear regime occurred for this condition, as observed in the friction force results. A mean value of wear rate was estimated from the linear regression of the total mass loss (pin and disk) for each replica. The wear rate results will be commented in the discussion section. The mass loss results agreed with those of friction, where an only steady state regime was observed.

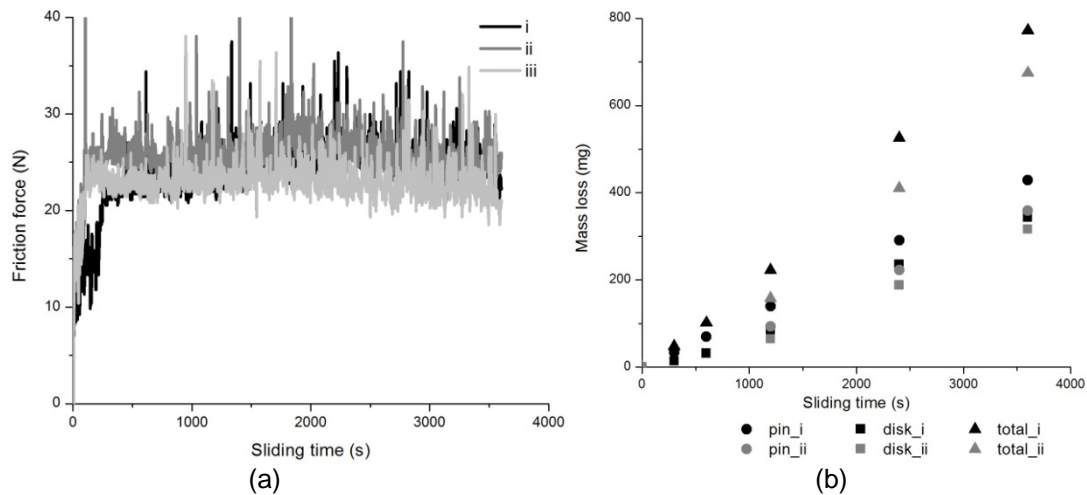


Figure 1. Friction force (a) mass loss (b) as a function of the sliding time for the *lph1.1* condition.

The curves of the friction force for the *lph1.2* condition are showed in Figure 2(a). After the running-in period, it can be seen a first steady state regime which was the same acting during the entire test for the *lph1.1* condition, with a mean value of friction force between 20 and 25 N. In sliding times between 2200 e 2500 s, a second steady state regime begins to operate, exhibiting a lower value and variation in the friction force. The mean value of friction force varied between 15 and 20 N. The lower variation in the friction force, in comparison with the first steady state regime, suggests a weaker interaction between the surface asperities. An increase in the disk hardness, from *lph1.1* to *lph1.2* condition, results in the presence of a second steady state regime.

In Figure 2(b) it can be seen the evolution of mass loss of bodies as a function of the sliding time. In spite of the differences between the mass losses of replicas, two periods of wear behavior can be noted. In the first one, an initially high wear rate is observed, in particular for the pins. On the other hand, a second period appears after 2400 s, in which the wear rate of sliding bodies is lower. In other words, the wear behavior represents the friction regime transition observed in **Erro! Fonte de referência não encontrada.** The increase in the disk hardness resulted in a wear regime transition, possibly from severe to mild wear.

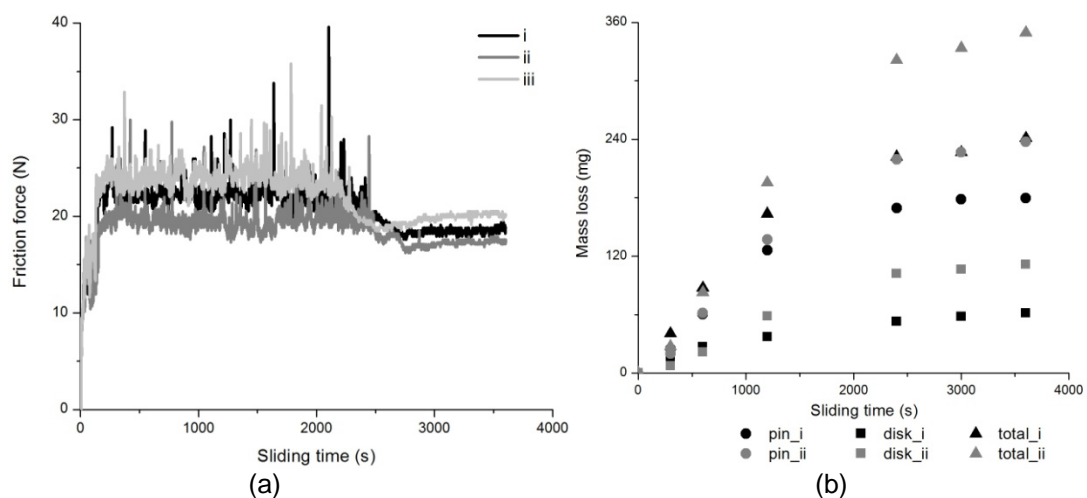


Figure 2. Friction force (a) mass loss (b) as a function of the sliding time for the *lph1.2* condition.

Figure 3 shows the curves of friction force for the *lph1.3* condition. This condition exhibits also a transition in the steady state regime. With the increase of the disk hardness (*lph1.3* condition), it was promoted a lower number and magnitude of friction force peaks in the first steady state. On the other hand, the critical sliding time for transition diminished, exhibiting values between 1540 e 1800 s. This result suggests that a transition in the steady state regime was accelerated by an additional increase of the disk hardness, from *lph1.2* to *lph1.3* condition.

3.2 High Pin Hardness

Figure 4(a) presents the curves of friction force as a function of sliding time for the *hph1.1* condition. In this condition, a first steady state regime appears after the running-in period, in which the friction force remains approximately constant (20 N) until sliding times between 700 and 800 s. At these sliding times, the friction force rapidly falls to values close to 18 N. In this way, a transition from a first to a second steady state regime occurs. As observed with the *lph1.2* and *lph1.3* conditions, the transition becomes evident by a decrease in the value and variation of the friction force.

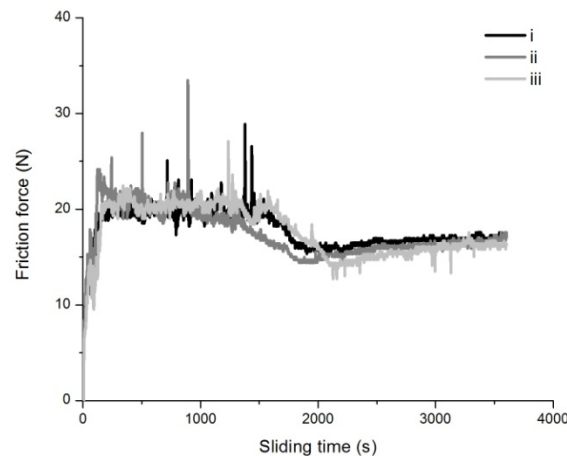


Figure 3. Friction force for the *lph1.3* condition.

Figure 4(b) presents the mass loss variation of the sliding bodies with the sliding time for the *hph1.1* condition. An equivalent behavior was achieved for both replicas in terms of curve inclination. The differences in the mass loss for each replica could be a consequence of the unpredictable running-in periods. A first wear regime is observed with high wear rate, which was present until sliding times between 1200 and 1800 s. After the sliding time for transition, a lower wear rate was found. This result agrees with the friction force curves, where a steady state transition occurs in sliding times between 600 and 900 s. A higher sliding time for transition in the mass loss results could be associated to the fact of interrupted tests involve new running-in periods every time that a sliding test was restarted. These running-in periods could change considerably the wear process of surfaces in comparison with the uninterrupted tests.

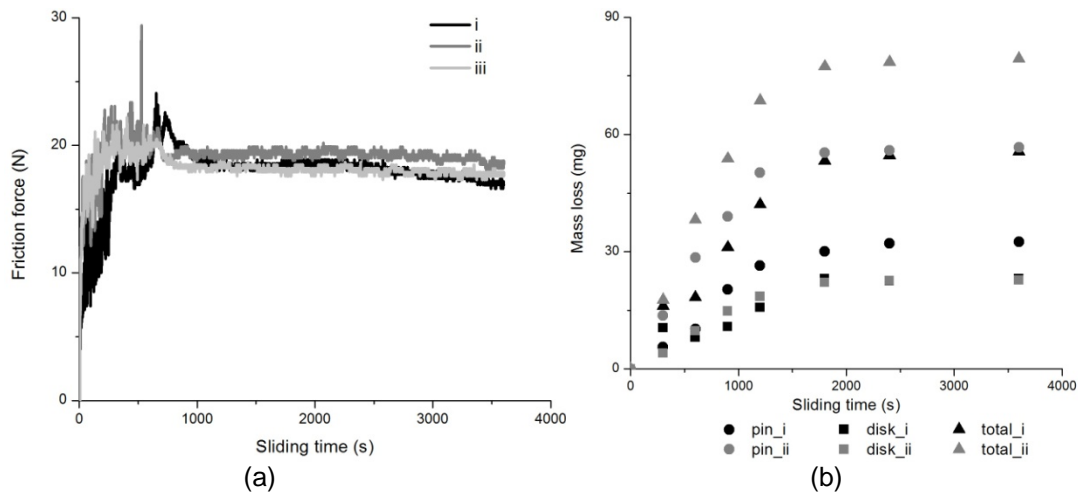


Figure 4. Friction force (a) mass loss (b) as a function of the sliding time for the *hph1.1* condition.

The curves of the friction force for the *hph1.2* condition are showed in Figure 5(a). In this case, after the running-in period, the friction force initially exhibits an increasing behavior until that a maximum value is achieved. In sliding times between 600 and 800 s, the friction force rapidly diminishes and remains approximately constant and close to 20 N. The latter behavior indicates the operation of a steady state regime, which corresponds to the second steady state regime observed in the *hph1.1* condition. This means that an increase of the disk hardness leads to inhibit the first steady state regime, which was found for the *hph1.1* condition.

The mass loss of sliding bodies as a function of the sliding time for the *hph1.2* condition is shown in Figure 5(b). This condition exhibited a similar behavior to the *hph1.1* condition, with a wear regime transition from a high to a low wear rate value. However, the sliding time for transition was between 900 and 1200 s for this condition. Then, an increase in the disk hardness accelerated the transition from severe to mild wear, as observed in the friction force curves of Figure 5(a).

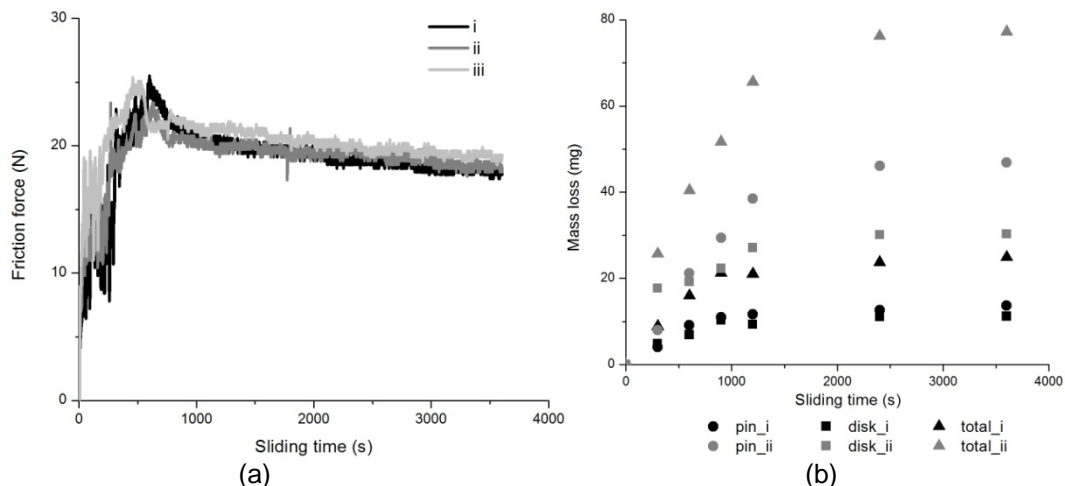


Figure 5. Friction force (a) mass loss (b) as a function of the sliding time for the *hph1.2* condition.

Figure 6 shows the curves of friction force for the *hph1.3* condition. This condition exhibits a similar behavior to the *hph1.2* condition, with a peak of the friction force being immediately achieved after the running-in period. As observed in the *hph1.2* condition, the friction force abruptly diminishes to remain approximately constant

(17 N). In this way, a mild wear regime predominantly acted during the entire test. This condition can be seen as the opposite behavior of the *lph1.1* condition, where only a severe wear regime with a high value and variation of friction force was observed.

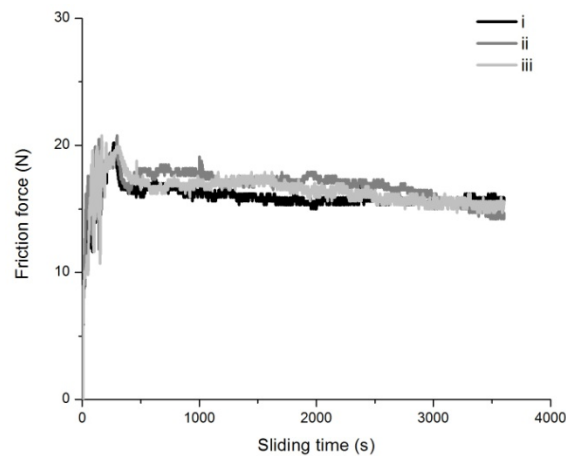


Figure 6. Friction force for the *hph1.3* condition.

3.3 Worn Surfaces Characterization

Figure 7 shows the images of pin worn surfaces for the *lph1.1* (a) and the *hph1.3* (b) conditions, which represent the surface characteristics of the severe and mild wear regimes, respectively. The pin surface for the *lph1.1* condition presents a bright appearance, together with plastic deformation traces as can be observed at the surface edges. This result suggests that a dominant wear mechanism of adhesion and plastic deformation took place for this condition. On the contrary, the pin surface of the *hph1.3* condition exhibits oxidation regions, without considerable traces of plastic deformation.

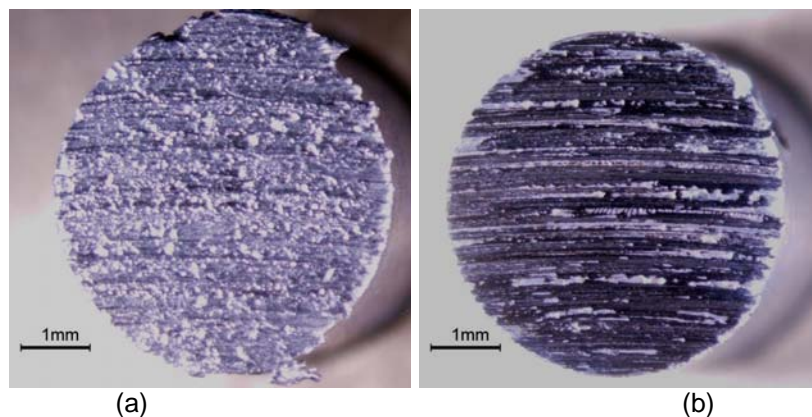


Figure 7. Images of pins worn surfaces for the *lph1.1* (a) and the *hph1.3* (b) conditions.

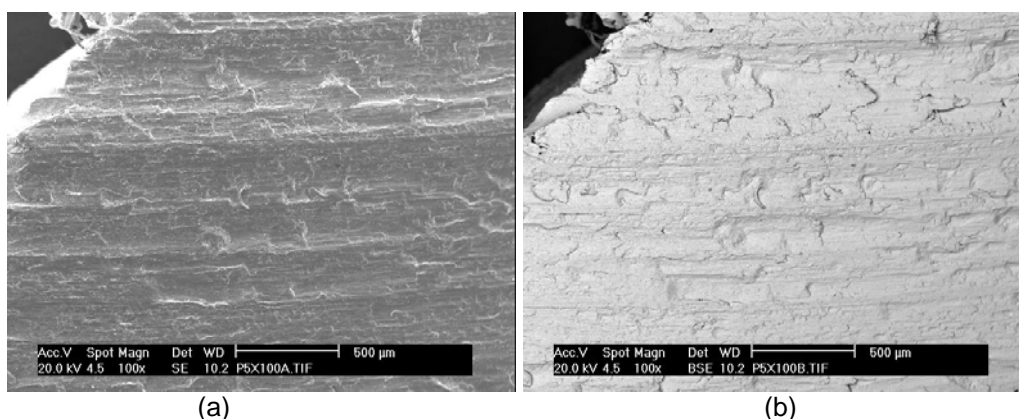
The SEM images of pins worn surfaces in secondary electrons and backscattered electrons modes for the *lph1.1* (a and b) and the *hph1.3* (c and d) conditions are displayed in Figure 8. The images for the *lph1.1* condition present adhesion and plastic deformation traces in the secondary electrons mode (a), but no presence of oxides was identified in backscatter electrons mode (b). On the other hand, an absence of plastic deformation can be noted for the *hph1.3* condition (c), and a presence of a preferably chemically different regions is observed (probably oxides) in the backscattered electrons mode image (d).

The roughness profiles of pins worn surfaces for the *lph1.1* (a) and the *hph1.3* (b) conditions are displayed in Figure 9. For the *lph1.1* condition, it can be seen a roughness profile with high peaks and low valleys, as confirmed by the R_q value. A smoother surface was obtained for the *hph1.3* condition, with a lower value of R_q . This result confirms that rougher surfaces are produced by the adhesive wear mechanism in comparison with the oxidative wear mechanism.

4 DISCUSSION

4.1 Low and High Pin Hardness Conditions

A summary of the friction and wear results for all test conditions are shown in Table 2. Initially, the sliding times for wear regime transition (t_{trans}) are listed, which were estimated from the friction force curves. The mean values of friction force (F_{f1} and F_{f2}) and wear rate (w_1 and w_2) estimated for the first and second wear regimes are also listed. Initially, it must be analyzed the low pin hardness conditions. For the lowest disk hardness condition (*lph1.1*), an only steady state regime was observed and it was the severe wear regime. The values for the friction force and the wear rate were only listed for the first wear regime and they were the highest values achieved between all test conditions. This can be explained by the action of the dominant adhesive wear mechanism, as revealed by the image and the roughness profile of the pin worn surface. With the increase of the disk hardness (*lph1.2* condition), a wear regime transition is achieved from severe to mild wear. The sliding times for transition were between 2220 and 2460 s. The transition was characterized by the diminution of the value and variation (standard deviation) of friction force. The mean value of wear rate ($19.7 \cdot 10^{-3}$ mg/s) for the mild regime was an order of magnitude lower than the wear rate ($219.9 \cdot 10^{-3}$ mg/s) for the *lph1.1* condition. A similar behavior to the *lph1.2* condition was found with an increase of the disk hardness (*lph1.3* condition), where a wear regime transition was also observed. In this case, the values of the sliding times for transition and of the friction forces in the two wear regimes decreased. In other words, an increase of the disk hardness accelerated the wear regime transition for lower sliding times.



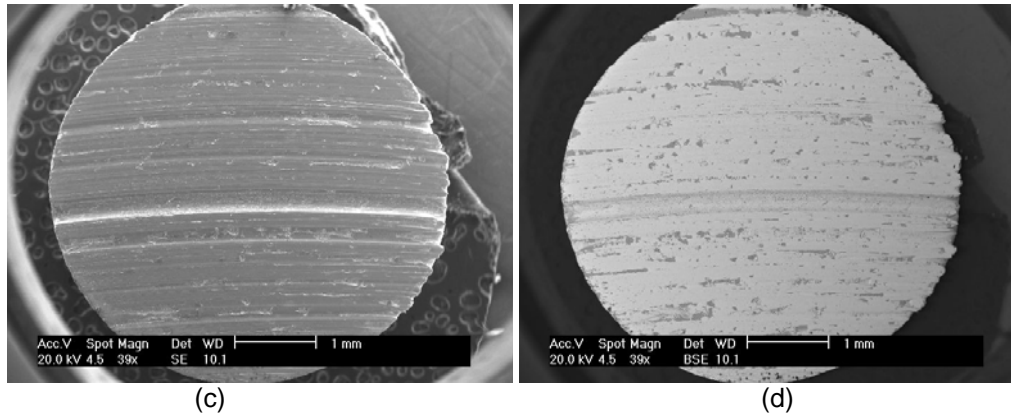


Figure 8. SEM Images of pin worn surfaces in secondary electrons and backscattered electrons modes for the *lph1.1* (a and b) and the *hph1.3* (c and d) conditions, respectively.

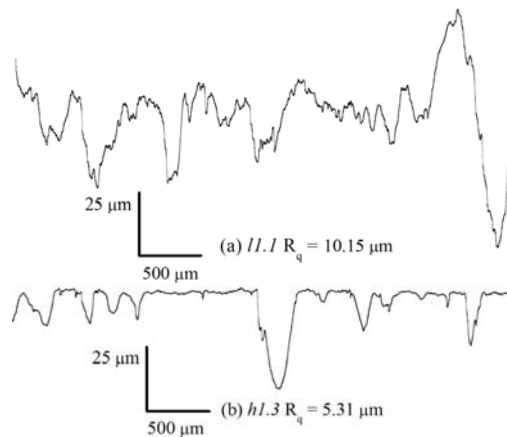


Figure 9. Roughness profiles of pins worn surfaces for the *lph1.1* (a) and the *hph1.3* (b) conditions.

Table 2. Friction and wear results for all test conditions

Test condition	t_{trans} [s]	Ff_1 [N]	Ff_2 [N]	w_1 [10^{-3} mg/s]	w_2 [10^{-3} mg/s]
<i>lph1.1</i>	-	24.5 ± 1.4	-	219.9 ± 6.3	-
<i>lph1.2</i>	2220-2460	21.9 ± 1.2	18.6 ± 0.6	-	19.7 ± 5.4
<i>lph1.3</i>	1540-1800	20 ± 1.2	16 ± 0.7	-	-
<i>hph1.1</i>	650-750	19.6 ± 0.4	18.2 ± 0.2	-	1.2 ± 0.1
<i>hph1.2</i>	550-650	22 ± 1.2	19.6 ± 0.6	-	3.2 ± 2.3
<i>hph1.3</i>	-	-	16.4 ± 0.5	-	-

For the conditions of the high pin hardness, an equivalent behavior to the low pin hardness conditions was observed. Initially, with the lowest disk hardness (*hph1.1* condition) a wear regime transition was found. The sliding times for transition were between 650 and 750 s and a decrease in the value of friction force was obtained after transition. The mean value of wear rate ($1.2 \cdot 10^{-3}$ mg/s) for the mild wear regime was two orders of magnitude lower than that of the severe wear regime of the *lph1.1* condition. An acceleration of the wear regime transition was promoted with the increase of the disk hardness (*hph1.2* condition), where lower sliding times for transition were found (550 to 650 s). Finally, an only steady state regime was observed for the *hph1.3* condition, where the severe wear regime was totally inhibited and only the mild wear regime operated. The image and roughness profile of the pin worn surface for this condition showed that probably an oxidative wear mechanism was responsible for the low wear rate of the sliding bodies.

4.2 Wear Regimes Characterization

The friction and wear results, together with the worn surfaces analysis, evidenced the operation of two different wear mechanisms: oxidative and adhesive wear. The action of these mechanisms promoted the mild and severe wear regimes, respectively. The characterization of both wear regimes was made in terms of friction, wear and appearance and roughness of worn surfaces.

The friction force curves constitute a first aspect to analyze the wear regimes operation. Taking as reference the test conditions where an only wear regime predominantly acted, *lph1.1* and *hph1.3* conditions, it can be seen that friction force values were different. The mild wear regime exhibited mean values below 20 N ($\mu_f \approx 0.6$) and a value near to 24 N ($\mu_f \approx 0.7$) was produced with the severe wear regime. This result agrees with previous investigations of Archard and Hirst,⁽¹⁾ who comment the little variation in the friction coefficient in spite of the change of some orders of magnitude in wear rate obtained with the wear regime transition. The results also agree with the maps of friction regimes proposed by Blau⁽²⁰⁾ and Bhushan,⁽²¹⁾ where higher values of friction coefficient are associated to the regime dominated by plastic deformation (severe wear) in comparison with the elastic contact regime (mild wear).

In relation to the friction force variation, standard deviations of 0.2 and 1.4 N were found for the mild and severe wear regimes, respectively. This behavior suggests that friction force variation is related with the magnitude of surface asperities interaction, where a higher magnitude is a consequence of plastic deformation and adhesion between sliding surfaces.⁽²²⁾ Another interpretation of friction force variation could be given by the stick-slip phenomena,⁽²¹⁾ where friction peaks are caused by adhesion joints formation that are later broken by the sliding of surfaces.

The characterization of worn surfaces confirmed the wear regime operation. For the severe wear regime, a metal-metal contact with adhesion and plastic deformation traces was found in the stereoscopy and SEM images. The mild wear regime was characterized by worn surfaces exhibiting probably oxides formation, which prevents the metallic contact between surfaces. This was verified by comparing the SEM micrographs in secondary and backscattered electron modes. In the same way, rougher surfaces were obtained with the adhesive wear mechanism in comparison with the smooth surfaces found for the oxidative wear mechanism. Measured R_q values seem to support this behavior. This wear regimes characterization agrees with that found in the classical works of Archard and Hirst,⁽¹⁻²⁾ Hirst and Lancaster,⁽³⁾ Welsh⁽¹³⁾ and in more recent works of Goto and Amamoto⁽⁴⁾ and Viáfara et al.⁽⁵⁾

4.3 Wear Regime Transitions

The wear regime transitions observed in the present results were those depending of one of the factor of the tribological system, the hardness of the sliding bodies, and of the sliding time. Initially, it can be analyzed the effect of the hardness of both sliding bodies. For this, a scheme based on the transitions map of Welsh⁽¹³⁾ was made, where the normal load applied (35 N) was assumed as being the T_1 critical transition load. This scheme is displayed in Fig. 10 and shows how with the decrease of the hardness of disk, from *hph1.2* to *hph1.1* condition, and of the pin, from *lph* to *hph* conditions, the severe wear regime was promoted. Similar results were obtained by Welsh,^(13,16) who used the same steel and hardness for both sliding bodies. This a very interesting result since the abrupt change in wear rate of sliding bodies was

achieved with a slight decrease of 27% of the pin hardness (from 436 to 318 HV) and of 23% of the disk hardness (from 460 to 356 HV).

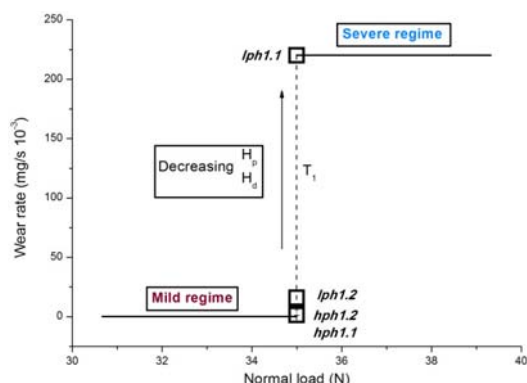


Figure 10. Scheme of the T_1 transition with the wear rates of the test conditions.

At the low pin hardness conditions, the transition from severe to mild wear regime with the increase of the disk hardness was still more critic. Even though the wear regime transition appeared in two thirds of the total sliding time, the mild wear regime was finally established. Then, with an increment of 9 % of the disk hardness (from 387 to 356 HV), a decrease in two orders of magnitude was achieved in wear rate of sliding bodies. The variation of wear rate as a function of the disk hardness for the low pin hardness conditions is shown in Figure 11(a). In this figure it can be seen that a decrease of the disk hardness results in a wear regime transition from mild to severe wear. There has been some works in which the effect of the harder sliding body on wear behavior was also studied.^(13,23) However, in these investigations there was not mention to the influence of the harder sliding body on wear regime transitions.

The wear regime transition in a critical sliding time must be also discussed. The variation of the sliding time for the severe/mild transition with the disk hardness can be seen in Figure 11(b). This figure shows that a decrease in the disk hardness increased the sliding time of the severe wear regime operation before of the mild wear regime being established. Previous works have been shown the variation of the critical sliding time for transition with some factors of the tribological system.^(7,12) Present results show that a slight variation of the hardness of the harder sliding body can dislocate the wear regime transition to lower or higher sliding times, which could be considerable during the performance of mechanical components.

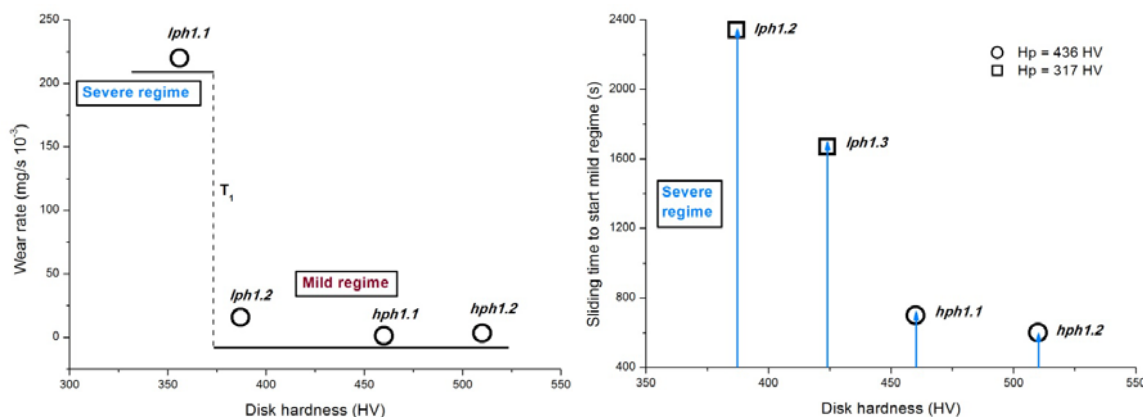


Figure 11. Variation of wear rate with the disk hardness for the low pin hardness conditions (a) and of the sliding time for severe/mild transition with the disk hardness (b).

The wear regime transitions being promoted by the variation of the disk hardness (the harder sliding body) is an outstanding result since main wear theories assume that only the material hardness of the softer body influences the wear behavior of the tribological system. In this work, it has been shown that a variation of the hardness of the harder can result in a wear regime transition, where a change of two orders of magnitude in wear rate is achieved. This noteworthy behavior could be seen as motivation to advance in better understand the origin of the sliding wear regime transitions of steels. A more detailed analysis of the present results will be made out in a future paper.⁽²⁴⁾

5 CONCLUSIONS

For the unlubricated sliding tests of pins of a low alloy steel against disks of a tool steel, wear regime transitions were obtained with the variation of the hardness of both sliding bodies. Higher values and variation of the friction force were found for the severe wear regime in comparison with the mild wear regime. The wear rates between both wear regimes differed by about two orders of magnitude. The mild wear regime was characterized by the oxides formation at the sliding surfaces, resulting in a dark smooth surface and a low value of R_q . On the other hand, a bright and rougher surface with adhesive and plastic deformation traces and a high value of R_q was obtained for the severe wear regime.

The wear regime transitions with the variation of the tribological conditions (hardness of sliding bodies) and of the sliding time were observed. A wear regime transition from mild to severe wear was found when the hardness of both disk and pin hardness were diminished. In the second kind of transition, for each condition of pin hardness, the decrease of the disk hardness results in the increase of the sliding time for transition, in which the severe wear operated before the mild wear being established. The effect of the hardness of the harder body is a result to highlight since the hardness of the softer body has been taken for a long time ago as the only property of sliding bodies to be considered to predict the wear behavior of the tribological system.

Acknowledgements

The authors greatly acknowledge the financial support offered by the Sao Paulo State Research Foundation (FAPESP) through the project 2005/59131-0 and the heat treatments provided by *Bodycote Brasimet* of Brazil.

REFERENCES

- 1 ARCHARD, J.F.; HIRST, W. The wear of metals under unlubricated conditions, **Proceedings of the Royal Society of London**, v. A236, p. 397-410, 1956.
- 2 ARCHARD, J.F.; HIRST, W. An examination of a mild wear process, **Proceedings of the Royal Society of London**, v. A238, p. 515-528, 1957.
- 3 HIRST, W.; LANCASTER, J.K. Surface film and metallic wear, **Journal of Applied Physics**, v. 27, p. 1057-1065, 1956.
- 4 GOTO, H.; AMAMOTO, G. Effect of varying load on wear resistance of carbon steel under unlubricated conditions, **Wear**, v. 253, p. 1256-1266, 2003.
- 5 VIÁFARA, C.C.; CASTRO, M.I.; VÉLEZ, J.M.; TORO, A. Unlubricated sliding wear of pearlitic and bainitic steels, **Wear**, v. 259, p. 405-411, 2005.

- 6 VIÁFARA, C.C.; SINATORA, A. Influence of hardness of the harder body on wear regime transition in a sliding pair of steels, **Wear**, v. 267, p. 425-432, 2009.
- 7 FARRELL, R.M.; EYRE, T.S. The relationship between load and sliding distance in the initiation of mild wear in steels, **Wear**, v. 15, p. 359-372, 1970.
- 8 IWABUCHI, A.; HORI, K.; KUBOSAWA, H. The effect of oxide particles supplied at the interface before sliding on the severe-mild wear transition, **Wear**, 128:123-137, 1988.
- 9 KATO, K. Severe-mild wear transition by supply of oxide particles on sliding surface, **Wear**, v. 255, p. 426-429, 2003.
- 10 KATO, K.; KOMAI, K. Tribofilm formation and mild wear by tribo-sintering of nanometersized oxide particles on rubbing steels surfaces, **Wear**, v. 262, p. 36-41, 2007.
- 11 KATO, K. Effect of supply of fine oxide particles onto rubbing steel surfaces on severe-mild wear transition and oxide film formation, **Tribology International**, v. 41, p. 735-742, 2008.
- 12 HIRATSUKA, K.; MURAMOTO, K. Role of wear particles in severe-mild transition, **Wear**, v. 259, p. 467-476, 2005.
- 13 WELSH, N.C. The dry wear of steels: I and II, **Philosophical Transactions of the Royal Society of London**, v. A257, p. 31-72, 1965.
- 14 LANCASTER, J.K. The influence of temperature on metallic wear, **Proceedings of the Physical Society of London**, v. B70, p. 112-118, 1957.
- 15 LANCASTER, J.K. The formation of surface films at the transition between mild and severe metallic wear, **Proceedings of the Royal Society of London**, v. A273, p. 467-483, 1963.
- 16 WELSH, N.C. Frictional heating and its influence on the wear of steel, **Journal of Applied Physics**, v. 28, p. 960-968, 1957.
- 17 OH, H.K.; YEON, K.H.; KIM, H.Y. The influence of atmospheric humidity on the friction and wear of carbon steels, **Journal of Materials Processing Technology**, v. 95, p. 10-16, 1999.
- 18 LIEW, W.Y.H. Effect of relative humidity on the unlubricated wear of metals, **Wear**, v. 260, p. 720-727, 2006.
- 19 VIÁFARA, C.C. **Transição no regime de desgaste por deslizamento dos aços: uma abordagem termodinâmica** (Sliding wear regime transition of steels: a thermodynamical approach). Doctoral Thesis (in Portuguese), Polytechnic School of the University of São Paulo, Brazil, 2010.
- 20 BLAU, P.J. **Friction, lubrication, and wear technology: from concepts to applications**, CRC Press, 1995.
- 21 BHUSHAN, B. **Introduction to tribology**, John Wiley and Sons, 2002.
- 22 BLAU, P.J. The significance and use of the friction coefficient, **Tribology International**, v. 34, p. 585-591, 2001.
- 23 BIAN, S.; MAJ, S.; BORLAND, D.W. The unlubricated sliding wear of steels: the role of the hardness of the friction pair, **Wear**, v. 166, p. 1-5, 1993.
- 24 VIÁFARA, C.C.; SINATORA, A. Unlubricated sliding wear of steels: An evaluation of mechanism responsible for the T₁ wear regime transition, submitted to the **18th International Conference on Wear of Materials**, 2011.